Swelling of Crosslinked Polyacrylates in Isotropic and Anisotropic Solvents

Tewfik Bouchaour,[1,2] Farida Benmouna,[2] Xavier Coqueret,[1] Mustapha Benmouna,[2] Ulrich Maschke[1]

[1]*Laboratoire de Chimie Macromoléculaire, CNRS (UPRESA 8009), Bâtiment C6, Université des Sciences et Technologies de Lille, F-59655 Villeneuve d'Ascq, France*
[2]*Laboratoire de Recherche sur les Macromolécules, Faculté des Sciences, Université Aboubakr Belkaïd, 13000 Tlemcen, Algeria*

Received 29 April 2002; accepted 2 December 2002

ABSTRACT: The purpose of this study was to examine the swelling and deswelling of photochemically crosslinked poly(*n*-butylacrylate) networks in isotropic and anisotropic solvents. The phase diagrams were established in terms of composition and temperature for five isotropic solvents, acetone, cyclohexane, methanol, tetrahydrofuran, and toluene, and two low-molecular-weight nematic liquid crystals, 4-cyano-4′-*n*-pentyl-biphenyl and an eutectic mixture of cyanoparaphenylenes. Networks were formed by ultraviolet curing in the presence of 0.5 wt % difunctional monomer (hexane diol-di-acrylate) and 0.5 wt % photoinitiator (Darocur 1173). Immersion in excess solvent allowed us to measure the solvent uptake by weight and to determine the size increase by optical microscopy in terms of temperature. We calculated weight and diameter ratios considering the swollen-to-dry network states of the samples. Phase diagrams were analyzed with the phantom network model according to the Flory–Rehner theory of rubber elasticity, and for the anisotropic solvents, modeling was supplemented with the Maier–Saupe theory of nematic order for free energy. The polymer–solvent interaction parameter was deduced as a function of temperature, but the values were in discrepancy with Fedors's model of solubility parameters, which overestimated the interaction. © 2003 Wiley Periodicals, Inc. J Appl Polym Sci 91: 1–9, 2004

Key words: photopolymerization; crosslinking; phase behavior; swelling; thermal properties

INTRODUCTION

The processes of network swelling and deswelling in low-molecular-weight solvents have been the subject of many intensive studies for several decades.[1–5] More than half a century ago, Flory and Rehner[6] developed a theory of rubber elasticity, suggesting that the swelling equilibrium is reached when the osmotic pressure of small solvent molecules that promote swelling is balanced by the elastic forces at the crosslinks opposing network strand extension. Many other theories were developed on the basis of a variety of arguments. For exemple, the concepts of scaling and the blob hypothesis suggested by de Gennes for polymers in strong solutions or in melts were extended to networks.[7–9] A large amount of data is available on these issues in the literature,[10–15] but the problem remains a subject of debate, attesting to its complexity and richness.

One of the pionering teams that contributed most decisively to the elucidation of the gel swelling/deswelling properties is the Massachusetts Institute of Technology team of Tanaka and coworkers. In 1973, Tanaka and colleagues[16,17] developed a theoretical formalism for gel dynamics using a continuum medium description and solving the corresponding diffusion equation. This approach was used successfully to rationalize the quasielastic light-scattering data from the gels. A few years later, Tanaka et al.[18] discovered the critical behavior of polyacrylamide gels in water–acetone systems. They demonstrated that the composition fluctuations drive the system toward criticality, whereby the light-scattering intensity diverges at a certain critical temperature. They showed for the first time that charged polyacrylamide gels in water–acetone can undergo tremendous volume changes by a change in the composition of the mixed solvent.[19,20]

These large volume changes observed under certain conditions when networks are immersed in selective solvents have triggered studies in different directions, leading to a variety of practical applications. The swelling properties of responsive gels are among the themes that retain the most attention nowadays. These systems undergo stretching and compression after small changes in conditions or as a response to external forces such as pressure, shear stress, electric field, or simply a change in pH or ionic strength of the charged gels. Another application which is currently of interest concerns the development of artificial mus-

Correspondence to: U. Maschke (maschke@univ-lille1.fr).

Journal of Applied Polymer Science, Vol. 91, 1–9 (2004)

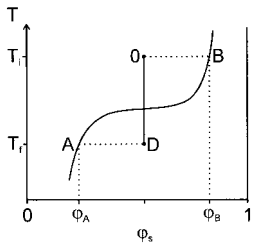

Figure 1 Hypothetical phase diagram showing the swelling process at a fixed temperature (path *OB*) and the cooling process resulting in the deswelling of the network (path OD). T_i, T_f, and φ_s represent the initial temperature, final temperature, and solvent volume fraction, respectively.

cles with crosslinked polymers having side-chain liquid crystalline groups.[21–26] The qualitative diagram in Figure 1 illustrates some features of the phase-separation processes, which involves the swelling and deswelling of polymer networks. Immersed in excess solvent at the temperature T_i, the network swells, and solvent uptake increases from O to B, where phase separation occurs. Any amount of solvent added beyond B goes to the pure solvent phase coexisting with a swollen network, which has a volume fraction $1 - \varphi_B$ of the polymer. Along path OD, the system undergoes cooling, which leads to a phase separation on contact with the solid line. Here, a homogeneous single-phase system undergoes a transition into a new state where a deswollen network of polymer volume fraction $1 - \varphi_A$ coexists with a pure solvent phase and T_f is the temperature at which the final equilibrium state is reached.

Interest in crosslinked polymers and low-molecular-weight liquid crystals (LMWLCs) is relatively new.[26–28] Crosslinked networks present substantial advantages over linear polymers by providing a higher mechanical strength and a better thermal stability. However, the challenge still remains to discover optimal systems combining these advantages with enhanced electrooptical performances and fast response times.[29,30] In this study, we aimed to study the swelling and deswelling properties of polymer networks in the presence of small molecules, including isotropic and nematic species exhibiting a selective miscibility with regard to the polymer. Systems made of ultraviolet (UV)-cured poly(*n*-butylacrylate) [poly(Abu)], five standards isotropic solvents, and two known nematic liquid crystals (LCs) were considered. A low concentration of crosslinker, the difunctional monomer hexane diol-di-acrylate (HDDA), was added because *n*-butylacrylate (Abu) is a mono functional monomer that alone would lead to linear chains. The low concentration of crosslinker yielded a loosely crosslinked network with more efficient swelling in good solvents than dense networks.

Swelling behavior depends on the solvent quality and the conditions of preparation (e.g., temperature and composition at crosslinking). By the proper choice of these conditions and materials, one should be able to control chain entanglements, minimize the number of network defects, and take advantage of the fluctuations that are frozen in by the crosslinking process. All of these aspects contribute to shape the physical properties of the network, affect its elasticity, and determine the concomittant phenomena of swelling and deswelling. It is clear that if crosslinking takes place under good solvent conditions, initial free chains are swollen and exhibit a relatively small number of self-entanglements. Under such conditions, no major defects, loops, or trapped entanglements should appear in the final products.

These considerations remain essentially valid if the small molecules are nematogens with some rearrangements required due to the nematic ordering. This work can be viewed as part of the systematic studies undertaken in our laboratory to explore the physical properties of composite materials made of polymers and LMWLCs such as polymer-dispersed liquid crystals (PDLCs).[27–30] Two main problems emerge when one deals with these materials with regard to their performances in terms of aging, thermal stability, mechanical strength, electrooptical responses, and relaxation processes. The miscibility of molecular constituents in the precursor mixture is the first problem. To characterize the specific features of the swelling behavior when small molecules are anisotropic, it is useful to undertake a comparative study with a model network in the presence of typical solvents and LCs. We combined two methods to analyze the swelling behavior. The first one consisted of weighting the network in its dry and swollen states and measuring the uptake of solvent at different temperatures. The amount of solvent absorbed increased with the degree of swelling and the extent of polymer–solvent interaction. In a good solvent, chain stretching was relatively large, whereas in a nonsolvent, stretching was rather low. Eventually chain collapse occurred via network contraction and rejection of the solvent as if it were squeezed. Swelling–deswelling phenomena induced large changes in the amount of solvent uptake with a significant modulation, depending on the temperature and polymer–solvent interaction.

The second method we used to characterize the swelling behavior was optical microscopy, which is particularly suitable for small samples in the submillimeter range. This is appropriate to systems with LCs where small quantities are usually used. These were two complementary methods that provided a good description of the swelling behavior of photocrosslinked poly(Abu)/HDDA networks in isotropic and nematic solvents versus temperature. To the best of our knowledge, such an investigation has not been reported before.

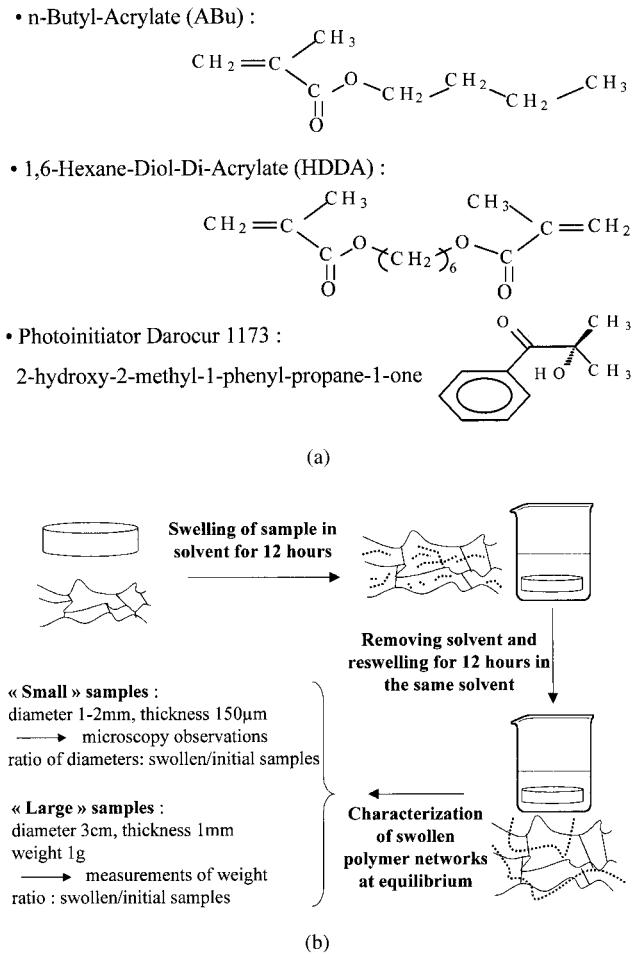

Figure 2 (a) Chemical structure of the components of the initial mixtures (prior to UV curing): Abu, HDDA, and Darocur 1173 and (b) experimental procedures: swelling, weighing, and optical microscopy.

EXPERIMENTAL

Materials

The chemical structures of the monofunctional monomer Abu, the difunctional crosslinker HDDA, and the photoinitiator Darocur 1173 (2-hydroxy-2-methyl + 1-phenyl-propane-1) are given in Figure 2(a). The monomer Abu was obtained from Aldrich, and HDDA was donated by Cray Valley (France). Five organic solvents of high purity (99%) were used as obtained from Aldrich. These were methanol, acetone, tetrahydrofuran (THF), toluene, and cyclohexane.

The LMWLCs 4-cyano-4′-*n*-pentyl-biphenyl (5CB) and E7 were purchased from Merck Eurolab GmbH (Germany). 5CB is characterized by the following transition temperatures: T_{CN} = 23°C and nematic-isotropic transition temperature (T_{NI}) = 35.3°C. The eutectic LMWLC mixture E7 contained 51 wt % 5CB, 25 wt % 4-cyano-4′-*n*-heptyl-biphenyl, 16 wt % 4-cyano-4′-*n*-oxyoctyl-biphenyl, and 8 wt % 4-cyano-4″-*n*-pentyl-*p*-terphenyl. Despite its multicomponent nature, E7 exhibited a single T_{NI} at 61°C.

Sample preparation

Abu/HDDA/Darocur mixtures were prepared at 99/0.5/0.5 wt % weight fractions and exposed to a UV lamp (Philips TL08) with a wavelength of 350 nm and an intensity of 1.5 mW/cm^2 under a nitrogen atmosphere. The exposure time was fixed to 15 min, although 5 min was sufficient to achieve a complete conversion of monomers. Initially, the samples exhibited a single homogeneous phase with uniformly distributed monomers and crosslinkers over the sample volume. The resulting polymer network was immersed in each solvent for a period of 12 h until it reached the final equilibrium state.

Techniques and experimental procedures

The experimental procedure is illustrated in Figure 2(b). Two series of samples with disc-like shapes were prepared. The first series corresponded to small samples, including the two mesogens, and were characterized by diameters in the range 1–2 mm and thicknesses near 150 μm. The swelling behavior of the samples was characterized by optical microscopy, which measured the ratio of swollen-to-dry sample diameters. The second series exhibited rather large diameters and thicknesses in the range of 3 cm for the diameter and 1 mm for the thickness. These samples were characterized by weight on the order of 1 g and by optical microscopy. For each solvent, the ratios of diameters and weights (swollen-to-dry states) were collected as a function of temperature. We considered four duplicate samples systematically to check reproducibility, and averaged values of the results were used in data analysis.

RESULTS AND DISCUSSION

A typical series of results with large samples of poly(Abu)/methanol is given in Figure 3. The averaged data of four duplicate samples were collected on the right hand side (RHS) at different temperatures. Similar results were obtained for other systems but are not shown here. Examples of images obtained at 20°C by optical microscopy in the dry and swollen states are given in Figure 4(a–d) for methanol [4(a,b)] and toluene [4(c,d)]. This figure shows some irregularities that appear as line segments and cusps. Such patterns on the surface of the gels undergoing high volume changes were reported by Tanaka [31,32] In our samples, a detailed investigation of patterns that could originate from the process of swelling and chain stretching were not accessible by the techniques available to us, and in any case, this investigation was not within the framework of this study. Here, we only aimed at illustrating the differences in network stretching in solvents exhibiting a high mismatch of miscibility

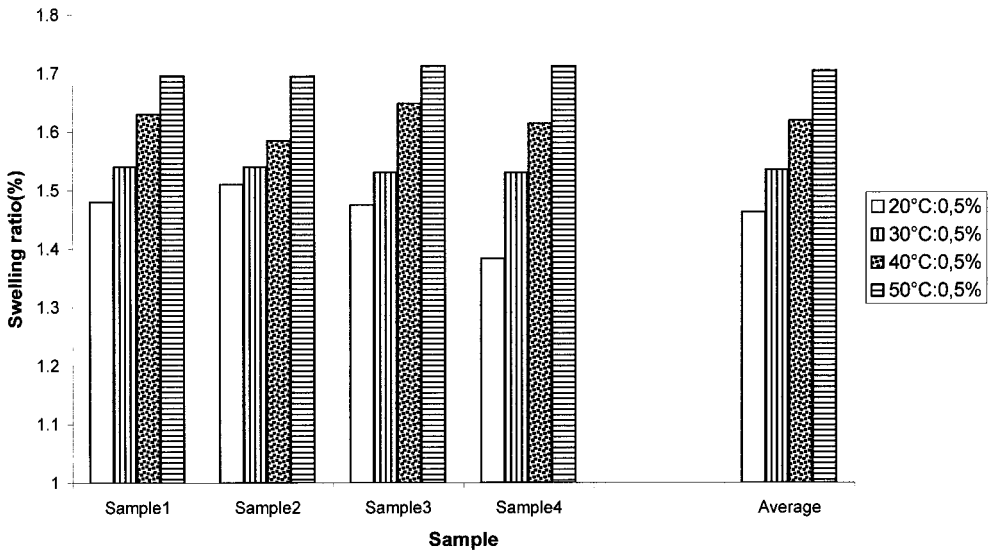

Figure 3 Swelling ratios of the poly(Abu)/HDDA/methanol system as a function of temperature. Four duplicates samples were used, and the averaged results are collected on the RHS of this figure.

with regard to the polymer. The polymer–solvent compatibility was primarily controlled by the Flory–Huggins[32] interaction parameter (χ) whether the small molecules were isotropic (standard solvent-like molecules) or anisotropic (LC molecules). The parameter χ depends on the nature of the molecular species in the system, the temperature, the degree of crosslinking of the polymer, and eventually, the composition. A detailed analysis of these effects was beyond the scope of this work. With regard to temperature effects, a direct evaluation of the solvent uptake and network swelling as a function of temperature is given in Figure 5. Consistent results were obtained by the two techniques that allowed weight and microscopy measurements. Toluene and THF exhibited the highest degree of swelling without noticable changes in the explored range of temperature. Although in these good solvents, the network reached its upmost swelling at room temperature, in methanol a low degree of swelling was found. The network diameter and solvent uptake on heating underwent a relatively high increase. In general, a large quantity of solvent was admitted inside the network, even though strand stretching remained moderate. Typical observations at room temperature were that weight ratios exceeded 6.0 in toluene and THF, and diameter ratios were less than 2.2. In methanol, the weight and diameter ratios were below 1. These tendencies were direct consequences of the polymer–solvent interaction.

Figure 5(b) includes data for 5CB and E7, which are located between those of cyclohexane and methanol. The miscibility of these LCs in poly(Abu) was slightly improved compared to the nonsolvent methanol but poorer than that of cyclohexane. The single component 5CB exhibited a better compatibility with poly(Abu) than E7, especially near 35°C. Below this temperature, the swelling ratio increased substantially in the presence of 5CB followed by a slight increase between 35 and 65°C. For E7, the swelling ratio increased more rapidly from 40°C and went from nearly 1.2 to 1.5 in this range. The nematic order seemed to enhance swelling, whereas in the isotropic case, the swelling of the network approached the saturation limit rather quickly.

Phase diagram

The case of isotropic solvents

According to Flory–Rehner theory,[6] the swelling of a polymer network reaches equilibrium when the osmotic pressure of the small molecules promoting swelling is balanced by the elastic forces at the crosslinks.

If isotropic swelling is assumed, the elongation (λ) is the same in all directions and is given by the ratio of the strand end-to-end distances before (R_0) and after (R) crosslinking. In the affine deformation model, one writes

$$\lambda^3 = \left(\frac{R}{R_0}\right)^3 = \left(\frac{\varphi_0}{\varphi_p}\right) \tag{1}$$

where φ_p is the polymer volume fraction in the swollen state and φ_0 is the corresponding quantity before crosslinking in the dry state.

An important issue in this context addresses the question of chain conformation in the deformed state and the appropriate model of the elastic free energy.

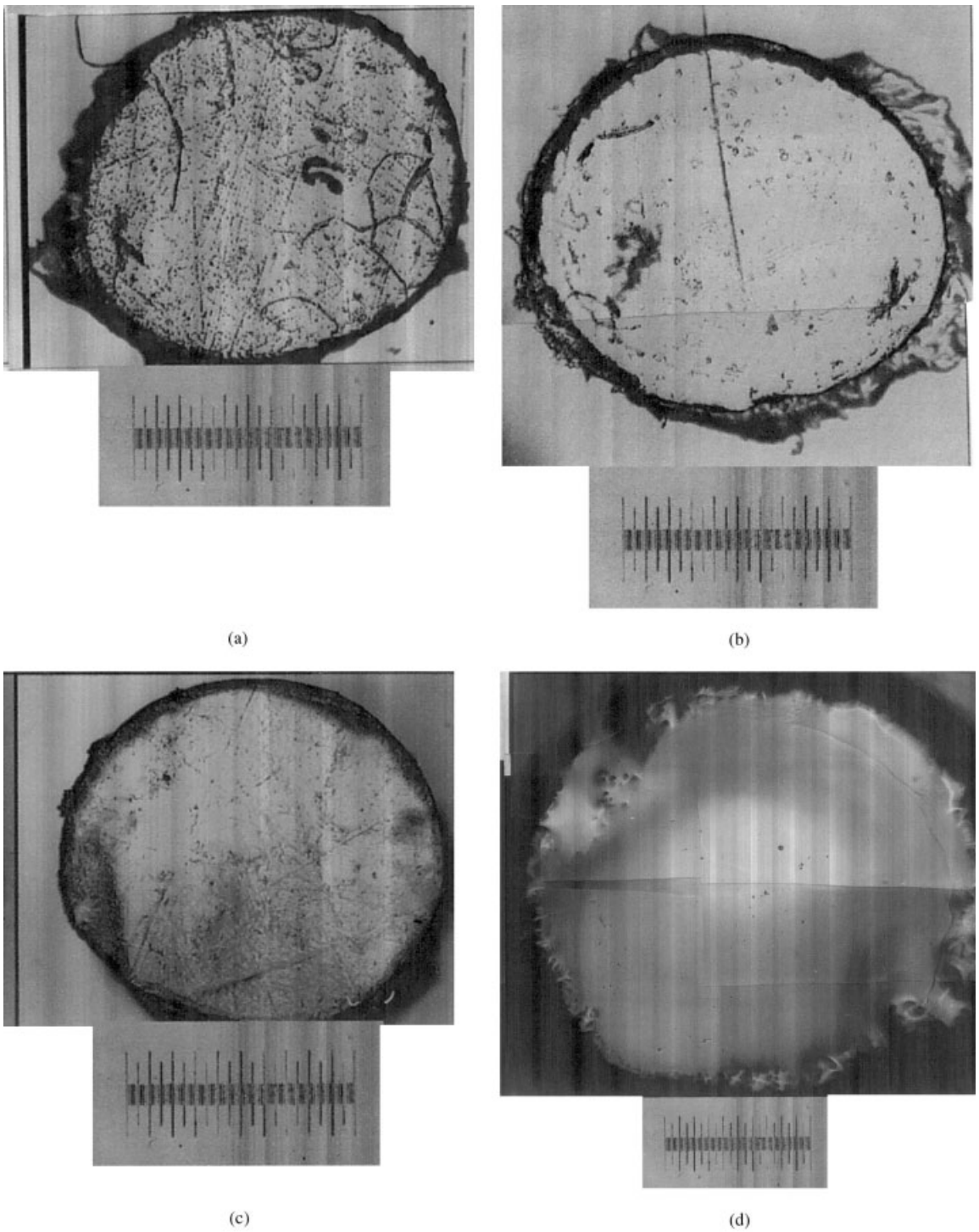

Figure 4 Camera pictures made during microscopy observations: (a) dry poly(*Abu*)/HDDA network used for swelling in methanol at 20°C, (b) swollen poly(N-Abu)/HDDA/methanol at 20°C, (c) dry poly(Abu)/HDDA network used for swelling in toluene at 20°C, and (d) swollen poly(Abu)/HDDA/toluene at 20°C. The scale in these pictures represents 100 μm between two consecutive large marks.

The neutron-scattering data of Bastide et al.[33] on polystyrene gels revealed only a small chain contraction, whereas the corresponding quantity of solvent expelled from the network was rather high. The reduction in the radius of gyration of the strands was below 10% for a degree of deswelling as high as 4.5. The affine deformation model predicts a chain contraction exceeding 25% for such deswelling.

Using the Flory–Rehner model, one can write the free energy as the sum of two terms, an elastic term

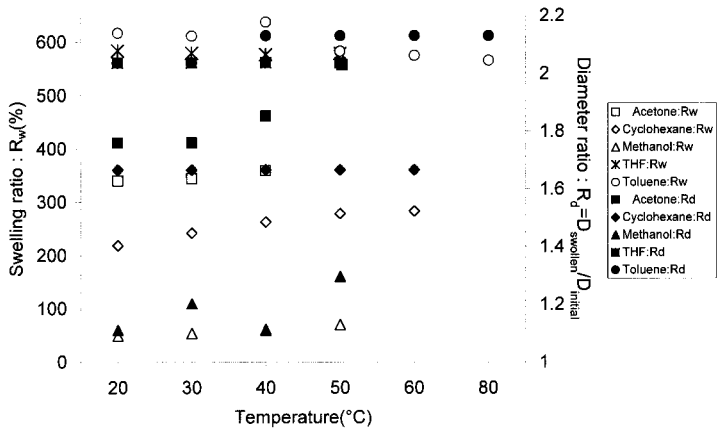

(a)

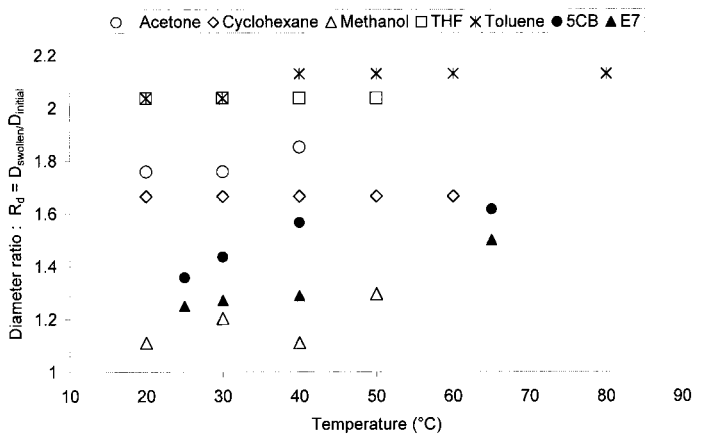

(b)

Figure 5 (a) Swelling ratios (swollen/dry) of weights (R_w's) and diameters (R_d's) for poly(Abu)/HDDA/solvent versus temperature. Different symbols are used to distinguish the results for each of the five solvents as indicated on the figure. These results showed that high solvent uptake led to small polymer streching. In most cases, only a small temperature variation was found. (b) The same as Figure 5(a) with R_d only and including the two nematic LCs 5CB and E7.

(f_{el}) and a mixing term (f_{mix}) given by eq. (2) and (3), respectively

$$\frac{f_{el}}{k_B T} = \frac{3\alpha \nu_e}{2} \varphi_0^{2/3}[\varphi_p^{-2/3} - 1] + \beta \nu_e \ln \varphi_p \qquad (2)$$

where k_B is the Boltzmann constant, T is the absolute temperature, and ν_e is the number of effective strands. This can be written in terms of φ_p and the number of segments between crosslinks (N_c) as $\nu_e = \varphi_p/N_c$. The elasticity parameters α and β are model dependent. The following models are often used: James–Guth[34] with $\alpha = 1$ and $\beta = 0$, the phantom network with $\alpha = (f - 2)/f$, and $\beta = 0$, the Flory affine model with $\alpha = 1$, and $\beta = 2/f$, and the Flory–Erman[35] junction fluctuation model with $\alpha = (f - 2)/f + (2\varphi_p/f)$, and $\beta = 2\varphi_p/f$, where f is the monomer functionality. Interestingly, if $f \to \infty$, the latter model yields the James–Guth prediction, whereas for $\varphi_p = 1$, it gives Flory's affine network result.[35]

The mixing free energy is

$$\frac{f_{mix}}{k_B T} = \varphi_s \ln \varphi_s + \chi \varphi_s \varphi_p \qquad (3)$$

where χ is the Flory–Huggins interaction parameter. These results were subject to the incompressibility condition $\varphi_p = 1 - \varphi_s$ and the fact that we were dealing with UV-cured samples in the absence of solvent where $\varphi_0 = 1$. On the basis of these considerations, one can calculate the phase diagram using the standard procedure of chemical potentials described previously.[27,28]

A theoretical fit of data gave us the parameter χ as a function of temperature for each system studied. Consistent with Flory's mean field approach, the affine deformation model yields the elastic parameters $\alpha = \beta = 1$ and takes into account the difunctionality of the crosslinker. In the this study, we used loosely crosslinked networks with $N_c = 100$. The numerical

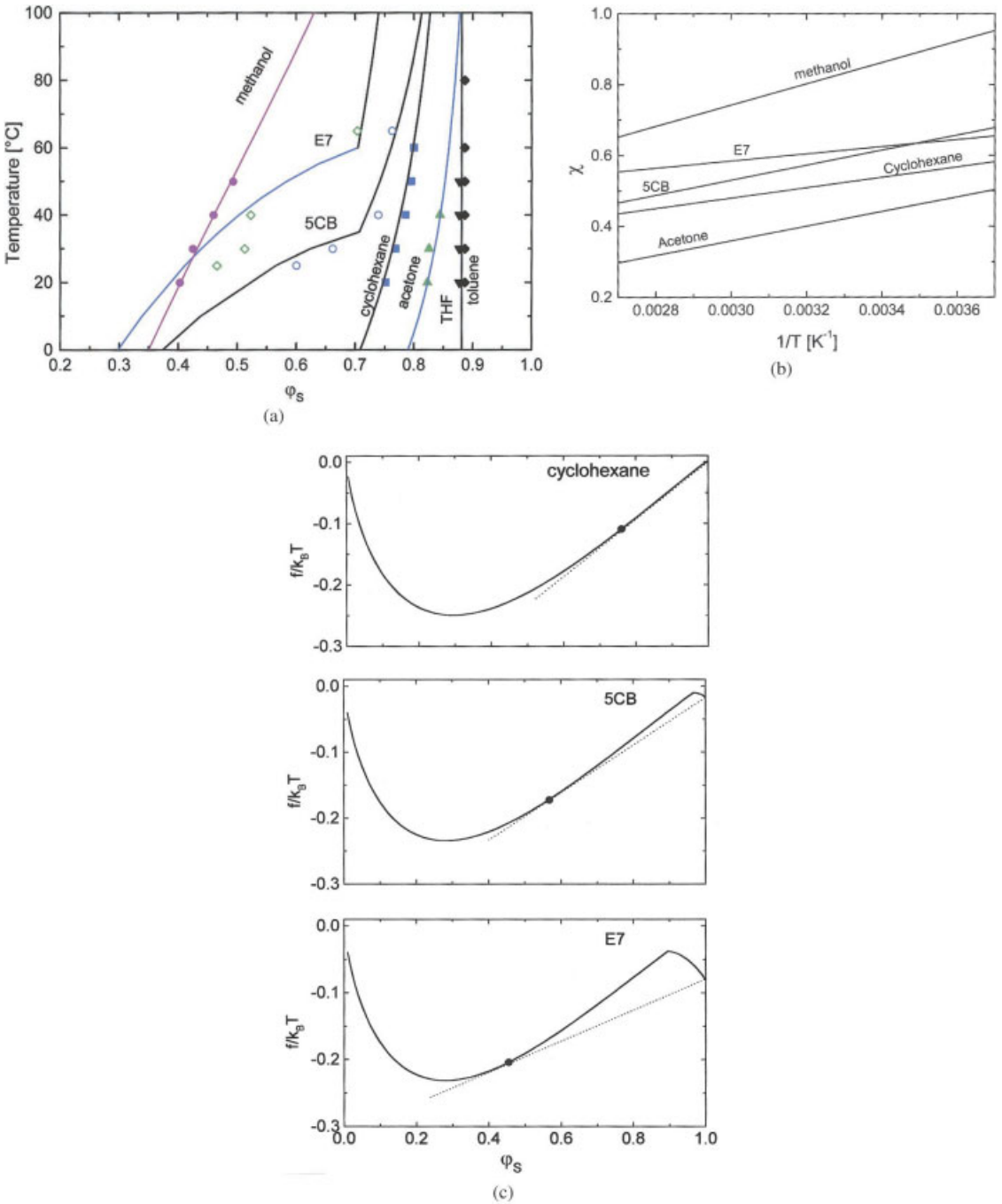

Figure 6 (a) Phase diagrams in the frame temperature versus φ_s for the systems involving the five isotropic solvents and the two nematic LCs. The symbols are experimental data, and the solid curves represent theoretical calculations as explained in the text. The parameters used to perform the calculations were $N_c = 100$, $\alpha = \beta = f = \varphi_0 = 1$. For the LCs, $T_{NI} = 35.3$°C for 5CB and 61°C for E7. The χ parameters were $0.0405 + 146.35/T$ (cyclohexane), $-0.26 + 206.35/T$ (acetone), -0.28 (toluene and THF), $-0.158 + 300/T$ (methanol), $-0.106 + 212/T$ (5CB), and $0.282 + 100.7/T$ (E7). (b) χ versus $1/T$ for the systems investigated as indicated on the figure. (c) Free-energy densities versus φ_s at 25°C for cyclohexane (upper curve), 5CB (middle curve), and E7 (bottom curve).

calculations yielded the solid curves of Figure 6(a). These plots were made in the same frame of temperature and φ_s deliberately to allow a direct comparison of the solvent quality on the swelling behavior and miscibility. On the left hand side (LHS), one finds the least compatible system, methanol/poly(Abu). Phase separation look place on addition only near 40% solvent at room temperature. As shown on the RHS, THF and toluene exhibited a relatively high miscibility up to 80% before phase separation occurred. Regardless of the polymer–solvent interaction, the network elasticity due to crosslinks imposed a limit to swelling

even at a relatively high temperature. Beyond this limit, any solvent added went to the solvent pure phase. Cyclohexane and acetone had intermediate miscibilities between methanol and THF.

The Flory–Huggins interaction parameters deduced from this analysis are given in Figure 6(b) as a function of $1/T$, where T is the temperature. Calculation of this parameter was made on the basis of the result of ref. 37: $\chi = -0.32 + v_s(\delta_s - \delta_p)^2/RT$, where v_s is the solvent molar volume, R the ideal gas constant, and δ_s and δ_p are the solubility parameters of the solvent and polymer, respectively. The latter parameter was computed according to Fedors[38] model from the chemical structure of the molecules, but the calculation led to overestimates of χ at room temperature for all of the solvents considered. Therefore, such a model was certainly not appropriate to our systems.

The case of nematic LCs

Anisotropic gel swelling was investigated by Onuki[39,40] starting from an expression of Ginsburg–Landau free energy in terms of the deformation tensor. He calculated explicitely the structure factor in the case of anisotropically deformed gels and tried to rationalize the butterfly pattern revealed by the neutron-scattering experiments.[41] Matsuyama et al.[42] reported a theoretical investigation of the volume phase transitions of gels in nematic LCs. They predicted that gels undergo a second-order phase transition at T_{NI} of the bulk LC and suggested that below this temperature, the gel is condensed. In the isotropic region above T_{NI}, a first-order volume phase transition was found. We also reported similar results[27,28]. In this article, we go along these lines and give data analyzed within an extension of the previous theoretical treatment to the case of LMWLCs. This extension was based on the mean field theory of Maier and Saupe[43,44] for the nematic order. According to this theory, the nematic free energy per unit volume is

$$\frac{f^{(n)}}{k_B T} = \frac{\varphi_s}{r_s}\left[-\ln Z + \frac{\nu\varphi_s S^2}{2}\right] \tag{4}$$

where ν the quadrupole interaction parameter and is inversely proportional to temperature

$$\nu = 4.54\,\frac{T_{NI}}{T} \tag{5}$$

where T_{NI} is the nematic–isotropic transition temperature of the LC and S is the nematic order parameter

$$S = \frac{1}{2}\left[3(\cos^2\theta) - 1\right] \tag{6}$$

where θ represents the angle between the LC director in the ordered domains and a reference axis Oz. Z is the nematic partition function

$$Z = \int_0^1 d\mu\, \exp\frac{m}{2}(3\mu^2 - 1) \tag{7}$$

where m is a mean field parameter that can be related to S and φ_s via the minimization of the free energy with respect to S. The result is

$$m = \nu\varphi_s S \tag{8}$$

Equation (4) is added to eqs. (2) and (3) to get the total free energy in this case. Besides this refinement, the rest of the procedure for establishing the phase diagram remained the same. The results of 5CB and E7 are included in Figure 6(a) for the sake of comparison. Note the emergence of the miscibility gap (N + I), whereby a swollen isotropic network coexisted with a pure nematic LC phase below T_{NI}. This transition temperature was not the same for 5CB and E7, meaning that the region N + I was wider in the latter case. The remarkable feature in comparison with isotropic solvents was the sudden change of the slope at T_{NI} due to the additional nematic term of eq. (4). Figure 6(c) shows three plots of the free energy versus concentration at 25°C. The dashed lines represent the double tangent from which one reads the compositions of the two coexisting phases in the miscibility gap. The upper curve shows the case of cyclohexane with no nematic order and a narrow gap (I + I). If 5CB were considered without the additional nematic term, one would get a similar plot as in the cyclohexane case. The nematic free energy introduced not only a drastic change in the curve above $\varphi_s = 0.92$ but also a significant shift to the LHS of the tangent point. In this case, the nematic interaction promoted phase separation significantly. This loss of miscibility was even more pronounced in the presence of E7, as one can see from the bottom curve of Figure 6(c).

CONCLUSIONS

The swelling and deswelling properties of poly(Abu)/HDDA crosslinked networks in the presence of low-molecular-weight solvent molecules, including nematogens, were investigated. The determination of the solvent uptake and the network size by weight and microscopy measurements permitted us to establish correlations between the quantity of solvent admitted in the network and concomittent strand stretching. The optical technique was particularly suitable for small-size samples and turned out to be decisive in the

case of LMWLCs, where small quantities are usually used.

By choosing solvents with a high selective miscibility in poly(Abu)/HDDA networks, we were able to evaluate the degree of swelling and deswelling via the measurement of the weight and diameter ratios in the swollen and dry states as a function of temperature. Consistent with the literature results, the uptake of solvent could be quite high, whereas strand stretching remained moderate. These aspects were modulated by the solvent–polymer interactions. For a nonsolvent such as methanol, both the weight and diameter ratios of swollen-to-dry networks remained moderate even after a significant increase in temperature. The rationalization of the results according to the Flory–Rehner theory of rubber elasticity led to χ. Fedors' model based on solubility parameters overestimated the polymer–solvent interaction under the conditions of these experiments.

The nematic interaction promoted phase separation into an isotropic swollen network and a nematic pure LC phase. These results were particularly useful for the establishment of a link between the swelling and deswelling behavior of crosslinked networks in LMWLCs. Advances achieved in understanding the rubber elasticity of polymer networks can be directly transmitted to PDLC systems that show promising signs for future applications in high-technology development techniques such as display and communication devices.

References

1. Broslow, W. Macromolecules 1971, 4, 742.
2. Wang, C.; Hu, Z.; Chen, Y.; Li, T. Macromolecules 1999, 32, 1822.
3. Johnson, R. M.; Mark, J. E. Macromolecules 1971, 5, 41.
4. Ilavsky, M.; Bonchal, K.; Dusek, K. Makromol Chem 1989, 190, 883.
5. Geissler, E.; Dupplessix, R.; Hecht, A. M. Macromolecules 1983, 16, 712.
6. Flory, P. J.; Rehner, R. J Chem Phys 1993, 11, 521.
7. Kavassalis, T. A.; Noolandi, J. Macromolecules 1989, 22, 2709.
8. Obukhov, S. P.; Rubinstein, M.; Colby, R. H. Macromolecules 1994, 27, 3191.
9. de Gennes, P. G. Scaling Concepts in Polymer Physics; Cornell University Press; Ithaca, NY, 1979.
10. Bastide, J.; Picot, C.; Candau, S. J Macromol Sci Phys 1981, 19, 13.
11. Rempp, P.; Herz, J.; Hild, G.; Picot, C. Pure Appl Chem 1975, 43, 77.
12. Gregonis, D. E.; Russel, G. A.; Andrade, J. D.; de Visser, A. C. Polymer 1978, 19, 1279.
13. Bastide, J.; Candau, S.; Leibler, L. Macromolecules 1981, 14, 719.
14. Colby, R. H.; Rubinstein, M. Macromolecules 1990, 23, 2753.
15. Zrinyi, M.; Horkey, F. Polymer 1987, 28, 1139.
16. Tanaka, T.; Hocker, L.O.; Benedek, G. B. J Chem Phys 1973, 59, 5151.
17. Shibayama, M.; Tanaka, T. Adv Polym Sci 1993, 109, 1.
18. Tanaka, T.; Ischimata, S.; Ishimoto, C. Phys Rev Lett 1977, 39, 474.
19. Tanaka, T. Phys Rev Lett 1978, 40, 820.
20. Hochberg, A.; Tanaka, T.; Nicoli, D. Phys Rev Lett 1979, 43, 217.
21. Pincus, P. Macromolecules 1976, 9, 386.
22. de Gennes, P. G. C R Acad Sci ser B 1997, 324, 343.
23. Kim, S. T.; Finkelmann, H. Macromol Chem Rapid Comm 2001, 22, 429.
24. Fischer, P.; Finkelmann, H. Progr Colloid Polym Sci 1998, 111, 127.
25. Park, B. D.; Lee, Y. S. React Funct Polym 2000, 44, 41.
26. Nwabunma, D.; Chiu, H. W.; Kyu, T. J Chem Phys 2000, 113, 6429.
27. Benmouna, F.; Maschke, U.; Coqueret, X.; Benmouna, M. Macromolecules 2000, 33, 1054.
28. Benmouna, F.; Maschke, U.; Coqueret, X.; Benmouna, M. Macromol Theory Simul 2000, 9, 215.
29. Drzaic, P. S. J Appl Phys 1986, 60, 2142.
30. Crawford, G. P.; Zumer, S. Eds., Liquid Crystals in Complex Geometries; Taylor & Francis: England, 1996.
31. Tanaka, T.; Sun, S. T.; Hirokawa, Y.; Katoyama, S.; Kucera, J.; Hirose, Y.; Amiya, T. Nature 1987, 325, 796.
32. Matuo, T.; Tanaka, T. J Chem Phys 1988, 89, 1695.
33. Flory, P. J. Introduction to Polymer Chemistry; Cornell University Press: Ithaca, NY, 1956.
34. Bastide, J.; Duplessix, R.; Picot, C.; Candau, S. Macromolecules 1984, 17, 83.
35. James, H.; Guth, E. J. J Chem Phys 1947, 15, 669.
36. Flory, P. J.; Erman, B. Macromolecules 1982, 15, 800.
37. Van Krevelen, D. W. Properties of Polymers; Elsevier: New York, 1990.
38. Fedors, R. F. Polym Eng Sci 1974, 14, 147.
39. Onuki, A. Adv Polym Sci 1993, 109, 61.
40. Onuki, A. J Phys 1992, 112, 45.
41. Mendes, E.; Lindner, P.; Buzier, M.; Boué, F.; Bastide, J. Phys Rev Lett 1991, 66, 1595.
42. Matsuyama, A.; Morii, R.; Kato, T. Mol Cryst Liq Cryst 1998, 312, 117.
43. Maier, W.; Saupe, A. Z Naturforsch A1959, 14a, 882.
44. Maier, W.; Saupe, A. Z Naturforsch A1960, 15, 287.